Journal of Sound and Vibration (2000) **237**(3), 395–410
doi:10.1006/jsvi.2000.3031, available online at http://www.idealibrary.com on IDEAL®

VIBRATION CONTROL OF VARIABLE THICKNESS PLATES WITH PIEZOELECTRIC SENSORS AND ACTUATORS BASED ON WAVELET THEORY

Y.-H. Zhou, J. Wang and X. J. Zheng

Department of Mechanics, Lanzhou University, Lanzhou, Gansu 730000, *People's Republic of China. E-mail: zhouyh@lzu.edu.cn*

AND

Q. Jiang

Department of Mechanical Engineering, University of California, Riverside, CA 92521-0425, *U.S.A.*

(*Received* 20 *October* 1999, *and in final form* 7 *April* 2000)

An approach of dynamic control for suppressing external disturbance to variable thickness beam plates with sensors and actuators of piezoelectric layers on/in the structures is proposed in this paper using the scaling function transform of the Daubechies wavelet theory for approximation of functions. By means of the generalized Gaussian integral to the scaling function transform, an expression of identification of deflection configuration of the structures is explicitly formulated by the electric charge/current signals measured from the piezoelectric sensors. After a control law of negative feedback of the identified deflection and velocity signals is chosen, the wavelet Galerkin method or wavelet weighted residual method is used to determine control voltage applied on the piezoelectric actuators. Due to that the scaling function transform is like a low-pass filter which can automatically filter out high order signals of vibration or disturbance from the measurement and the controller employed here, this control approach does not lead to the undesired phenomenon of control instability that is often generated in a control system and caused by the spilling over of high order signals from interaction between the measurement and the controller if no special techniques is used in the control system. Finally, a numerical simulation is carried out to show the efficiency of the proposed approach.

1. INTRODUCTION

With extensive applications of piezoelectric materials in engineering, the importance for research of piezoelectric materials has been considerably intensified in both engineering and theory. One application using piezoelectricity is to design an intelligent structure with control system of piezoelectric sensors and actuators to suppress an external disturbance in, e.g., space structures, antennas, rotor systems, and high-precision systems, etc. (see references [1–8], for example). In this area, most researchers concentrated their attention on how to design an efficient control system with a measurement sub-system of sensing and a controller sub-system of actuating by a mathematical program. For example, Lee [7] proposed an approach using continuously distributed piezoelectric sensors/actuators, while Sun *et al.* [8] established another approach using distributed piezoelectric elements on the basis of the technique of modal analysis of vibrations. The development of a finite element approach to piezoelectric structures was introduced in reference [1]. It is found that the

0022-460X/00/430395 + 16 $35.00/0

phenomenon of spilling over of high order signals can automatically be avoided in the system with continuously distributed piezoelectric sensors/actuators [7]. Its applications in vibration control are, however, still limited to very simple structures because it is too difficult to practically implement an effective sensor/actuator distribution for a complex structure and because the effectiveness of a sensor/actuator distribution highly depends on the vibration mode to be controlled. For the control system with distributed piezoelectric elements, identification of deflection of structures is performed by a system of linear algebraic equations that determine those modal co-ordinates employed in the modal analysis. However, it is not generally guaranteed that the coefficient matrix of the system is non-singular, and hence there is possibility in the system to fail an identification of deformation of structures such that the control system would lose its function.

The wavelet theory is one of the relative recent and powerful mathematical tools [9–11]. It has been found that the wavelet theory can be used for decomposition and reconstruction of a signal process, approximation of a function, and solving a boundary-value problem, etc. [11]. Due to that most of wavelet theories are generated by a numerical program, it is found that the accuracy of approximation of a function mainly relies upon a numerical approach of integral in the decomposition of the scaling/wavelet function transform.

In this paper, we will propose an approach of vibration control to variable thickness beam-type plates with piezoelectric sensors and actuators by the aid of the Daubechies wavelet theory. Once the piezoelectric layers on the beam plates are discretized at the nodes of the wavelet theory, first of all, an explicit expression of identifying deflection state of the plates are formulated by the electric charge/current measured from the piezoelectric sensors. By taking a control law of negative feedback of the identified signals of deflection and its velocity, secondly, the wavelet Galerkin/or weighted residual method is used to determine the distribution of control voltage applied on piezoelectric actuators. Finally, a numeric program of this control approach is developed to simulate the control process of the plates.

2. GOVERNING EQUATIONS

Consider a beam-type plate of length L, unit width and smoothly variable thickness. And assume that the piezoelectric layers of constant thickness h_p, such as PVDF, are attached on/in the top and bottom surfaces of the plate as sensors and actuators (see Figure 1). Taking the Cartesian co-ordinate system in which the co-ordinate plane oxy is coincident with the mid-plane of the plate and the z-axis is along the transverse direction of the plates, we denote by $h_b^*(x) \in C^1[0, L]$ the variation part of thickness of the plate. That is, the thickness of plate is $h_0 + h_b^*(x)$ in which h_0 is a referenced thickness. After the plate is considered to be symmetric about its mid-plane geometrically, the co-ordinates of surface of the plate and layers in the z direction are measured by

$$z_3 = -z_0 = h_p + (h_0 + h_b^*(x))/2, \qquad z_2 = -z_1 = (h_0 + h_b^*(x))/2. \tag{1, 2}$$

According to the laminated theory of piezoelectric plates [7], we can write the equivalent density of mass ρ, the equivalent thickness h, and the equivalent deflection rigidity D as follows:

$$\rho h = \sum_{i=1}^{3} \rho_i (z_i - z_{i-1}), \qquad D = \frac{1}{3} \sum_{i=1}^{3} \frac{Y_i}{1 - \mu_i^2} (z_i^3 - z_{i-1}^3) \tag{3, 4}$$

in which $\rho_1 = \rho_3$, $Y_1 = Y_3$ and $\mu_1 = \mu_3$ are the density of mass, the Young modulus, and the Poison ratio of the piezoelectric layers respectively; ρ_2, Y_2 and μ_2 are the density of mass, the

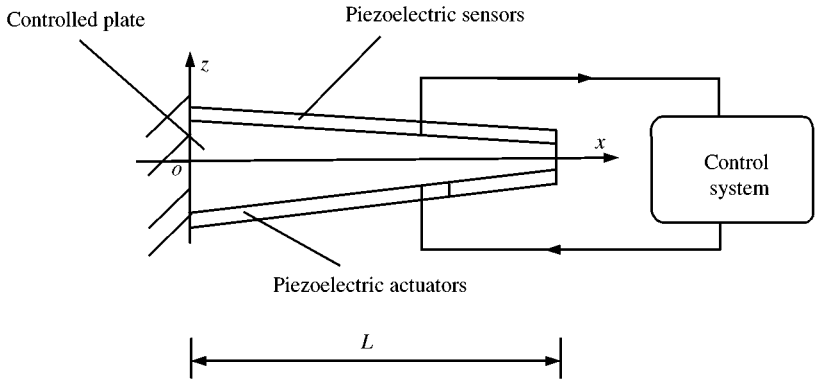

Figure 1. Schematic drawing of a variable thickness cantilever beam plate with piezoelectric sensors and actuators.

Young modulus, and the Poison ratio of the plate respectively. Once we substitute equations (1) and (2) into equations (3) and (4), one can find that the quantities ρ, h and D can be expressed by

$$D(x) = D_0 + D^*(x), \qquad \rho(x)h(x) = \rho_0 h_0 + \rho^*(x)h^*(x), \tag{5}$$

where $\rho_0 h_0$ and D_0 are the parts of equations (3) and (4) when $h_b^*(x) \equiv 0$, while $\rho^*(x)$ $h^*(x) = \rho(x)h(x) - \rho_0 h_0$ and $D^*(x) = D(x) - D_0$ are mainly related to $h_b^*(x)$. After that, we can write the deflection equation of the variable thickness plates with piezoelectric layers in the form

$$\frac{\partial^2}{\partial x^2}\left\{[D_0 + D^*(x)]\frac{\partial^2 w}{\partial x^2}\right\} + [\rho_0 h_0 + \rho^*(x)h^*(x)]\frac{\partial^2 w}{\partial t^2} = f(x,t), \quad 0 < x < L \tag{6}$$

with boundary conditions of, e.g., a cantilevered beam plate as shown in Figure 1,

$$w|_{x=0} = 0, \qquad \left.\frac{\partial w}{\partial x}\right|_{x=0} = 0, \tag{7}$$

$$\left.\frac{\partial^2 w}{\partial x^2}\right|_{x=L} = 0, \qquad \left.\frac{\partial^3 w}{\partial x^3}\right|_{x=L} = 0. \tag{8}$$

Here, $w = w(x, t)$ represents the deflection function of plate at instant t; $f(x, t)$ is the control force of equivalent transverse force generated from the control voltage applied on piezoelectric actuators. Let $V = V(x, t)$ the distribution of control voltage. As same as done in Lee [7], we have the relation of the control force to $V(x, t)$:

$$f(x,t) = -e_{31}\frac{\partial^2\{[r_{a0} + r_a^*(x)]V(x,t)\}}{\partial x^2} \tag{9}$$

in which $r_a(x) = r_{a0} + r_a^*(x)$ is the z-co-ordinate of piezoelectric actuator measured from the mid-plane at point x, while r_{a0} is the part of $r_a(x)$, i.e., the z-co-ordinate of the actuator at the reference point of h_0; and e_{31} represents the piezoelectric constant of the actuators or sensors.

Let $\Omega_k = [x_{k-1}, x_k]$ $(k = 1, 2, \ldots, M)$ be the regions occupied by piezoelectric elements. When the plate is deflected with $w = w(x, t)$ at instant t, the electric charge $q_k(t)$ and electric current $I_k(t)$ measured from the kth piezoelectric sensor can be formulated by Lee [7]

$$q_k(t) = -e_{31}\int_{\Omega_k}[r_{s0} + r_s^*(x)]\frac{\partial^2 w}{\partial x^2}\,\mathrm{d}x, \tag{10}$$

$$I_k(t) = \frac{\mathrm{d}q_k}{\mathrm{d}t} = -e_{31}\int_{\Omega_k}[r_{s0} + r_s^*(x)]\frac{\partial^3 w}{\partial x^2 \partial t}\,\mathrm{d}x. \tag{11}$$

Here, $r_s(x) = r_{s0} + r_s^*(x)$ denotes the distance from the mid-plane of plate to the piezoelectric sensors at point x, while r_{s0} is the z-co-ordinate of the sensor at the reference point of h_0.

In order to simplify the discussions later, here, we introduce the following dimensionless quantities:

$$\bar{w} = w/L, \qquad \bar{x} = x/L, \qquad \bar{t} = t/(\sqrt{\rho_0 h_0 L^4/D_0}), \qquad \bar{V} = V\Big/\left(\frac{D_0}{e_{31} r_{a0} L}\right),$$

$$\bar{q} = q/(e_{31} r_{s0}), \qquad \bar{\Omega}_k = [\bar{x}_{k-1}, \bar{x}_k], \qquad \bar{D}^* = D^*(x)/D_0, \tag{12}$$

$$g^*(x) = \rho^*(x)h^*(x)/(\rho_0 h_0), \qquad \bar{r}_a^* = r_a^*(x)/r_{a0}, \qquad \bar{f} = fL^3/D_0.$$

Then equations (6)–(11) are non-dimensionlized in the form

$$\frac{\partial^2}{\partial \bar{x}^2}\left[(1 + \bar{D}^*(\bar{x}))\frac{\partial^2 \bar{w}}{\partial \bar{x}^2}\right] + (1 + \bar{g}^*(\bar{x}))\frac{\partial^2 \bar{w}}{\partial \bar{t}^2} = \bar{f}(\bar{x}, \bar{t}), \quad 0 < \bar{x} < 1, \tag{13}$$

$$\bar{x} = 0: \quad \bar{w} = \frac{\partial \bar{w}}{\partial \bar{x}} = 0, \tag{14}$$

$$\bar{x} = 1: \quad \frac{\partial^2 \bar{w}}{\partial \bar{x}^2} = \frac{\partial^3 \bar{w}}{\partial \bar{x}^3} = 0, \tag{15}$$

$$\bar{f}(\bar{x}, \bar{t}) = -\frac{\partial^2[(1 + \bar{r}_a^*(\bar{x}))\bar{V}(\bar{x}, \bar{t})]}{\partial \bar{x}^2}, \tag{16}$$

$$\bar{q}_k(\bar{t}) = -\int_{\bar{\Omega}_k}[1 + \bar{r}_s^*(\bar{x})]\frac{\partial^2 \bar{w}}{\partial \bar{x}^2}\,\mathrm{d}\bar{x}, \quad k = 1, 2, \ldots, M, \tag{17}$$

$$\bar{I}_k(\bar{t}) = -\int_{\bar{\Omega}_k}[1 + \bar{r}_s^*(\bar{x})]\frac{\partial^3 \bar{w}}{\partial \bar{x}^2 \partial \bar{t}}\,\mathrm{d}\bar{x}, \quad k = 1, 2, \ldots, M. \tag{18}$$

When the plate is disturbed by deflection $w(x, t)$ and velocity $\dot{w}(x, t)$, the electric charges q_k and electric currents I_k will be generated on the piezoelectric sensors, which are given by equations (17) and (18). The applied control voltage across the piezoelectric actuators are dependent on a control law employed and the measurable signals. That is to say, an appreciate control law have to be taken to feed the measurable signals to the piezoelectric actuators through applying voltages $V(x, t)$ across the actuators, which leads to the change of deflection similar to the action of an equivalent transverse force of equation (16). In the

following sections, we will introduce an approach of the control including the identification of deflection of the plates in terms of the measurable charges and currents on the sensors, and the determination of control voltage distribution on the basis of the Daubechies wavelet.

From here on, we use only the dimensionless variables and parameters in the theoretical analysis. For simplicity, we will drop the bar over each dimensionless quantity. For example, we denote $\bar{w}$ by w, etc.

3. ESSENTIALITY OF WAVELET THEORY EMPLOYED

In this section, for the convenience of discussion, we briefly cite some elemental results of the Daubechies wavelet which we will use. The scaling function $\phi_N(x)$ of the Daubechies wavelet is defined in the support region $[0, 2N-1]$ in which N is an integer no less than 2, and $\phi_N(x)$ is numerically generated at the dyadic points $(j/2^n)(j = 0, 1, \ldots, (2N-1)2^n)$ (see reference [9]). After that, the base scaling functions $\phi_{n,k}(x)$ are defined by

$$\phi_{n,k}(x) = 2^{n/2}\phi_N(2^n x - k), \quad n, k \text{ integers.} \tag{19}$$

For a function $f(x) \in L^2(R)$, the scaling function transform with n-level can be written as

$$T_n f(x) = \sum_{k=k_1}^{k_2} a_{n,k}\phi_{n,k}(x) \tag{20}$$

in which the decomposition coefficients $a_{n,k}$ are given by

$$a_{n,k} = \langle f(x), \phi_{n,k}(x)\rangle = \int_{-\infty}^{\infty} f(x)\phi_{n,k}(x)\,\mathrm{d}x. \tag{21}$$

Here, k_1 and k_2 are integers dependent upon the region of function $f(x)$. For example, if $f(x)$ is defined in $[0, 1]$, we have $k_1 = 1 - 2N$ and $k_2 = 2^n$. It has been known that the scaling function transform of equation (20) functions like a low-pass filter. When n is sufficiently large, the scaling function transform is approximately equal to $f(x)$ itself (see reference [9]), that is

$$f(x) \approx T_n f(x) = \sum_{k=k_1}^{k_2} a_{n,k}\phi_{n,k}(x). \tag{22}$$

It could be found that the accuracy of the approximation is dependent on the numerical integral employed in equation (21). In order to enhance the accuracy, Wang and Zhou [12] proposed a generalized Gaussian integration with weighted functions $\phi_N(x)$ or $\phi_{n,k}(x)$ in the form

$$\int_0^{2N-1} f(x)\phi_N(x)\,\mathrm{d}x \approx \sum_{m=0}^{i} A_m f(x_m^*). \tag{23}$$

Here, A_m and x_m^*, which are independent of function $f(x)$, stand for the weighted coefficients and the nodes of the Gaussian integration respectively. According to equation (18), (21) and (23), and noting the support region of $\phi_N(x)$, one can get

$$a_{n,k} = \int_{k2^{-n}}^{(k+2N-1)2^{-n}} f(x)\phi_{n,k}(x)\,\mathrm{d}x = 2^{-n/2}\sum_{m=0}^{i} A_m f\left(\frac{x_m^* + k}{2^n}\right). \tag{24}$$

Further, the approximation of $f(x)$ is formulated in terms of $\phi_{n,k}(x)$ in the form

$$f(x) \approx 2^{-n/2} \sum_{k=k_1}^{k_2} \sum_{m=0}^{i} A_m f\left(\frac{x_m^* + k}{2^n}\right) \phi_{n,k}(x). \tag{25}$$

For the most simple form that $i = 1$, i.e., the algebraic accuracy of order 3, the weighted coefficients A_0, A_1 and the node x_1^* of the generalized Gaussian integration given in equation (23) have the following approximated expressions:

$$A_0 \approx 0, \quad A_1 \approx 1, \quad x_1^* \approx \int_0^{2N-1} x \phi_N(x)\, \mathrm{d}x. \tag{26}$$

In this case, equation (23) is reduced into

$$f(x) \approx 2^{-n/2} \sum_{k=k_1}^{k_2} f\left(\frac{x_1^* + k}{2^n}\right) \phi_{n,k}(x). \tag{27}$$

It is shown in reference [12] that the error of the generalized Gaussian integration to equation (21) for $i = 1$ decreases with $2^{-(4+1/2)n}$.

4. IDENTIFICATION OF DEFLECTION FROM SENSING

Take the elements of piezoelectric sensors and actuators to be coincident with the subregions of the wavelet theory, that is, $\Omega_k = [x_{k-1}, x_k]$ $(x_k = k2^{-n}, k = 1, 2, \ldots, 2^n)$ with $x_0 = 0$. Denote

$$H(x, t) = -\int_0^x [1 + r_s^*(x)] \frac{\partial^2 w}{\partial x^2}\, \mathrm{d}x. \tag{28}$$

According to equations (17) and (28), we get

$$H(x_k, t) = \sum_{m=1}^{k} q_m(t) \tag{29}$$

and

$$\frac{\partial H(x, t)}{\partial x} = -[1 + r_s^*(x)] \frac{\partial^2 w}{\partial x^2} \tag{30}$$

or

$$\frac{\partial^2 w}{\partial x^2} = -\frac{1}{1 + r_s^*(x)} \frac{\partial H(x, t)}{\partial x}. \tag{31}$$

Integrating equation (31) with respect to x and considering $H(0, t) = 0$ from equation (28), we get

$$\begin{aligned} \frac{\partial w(x, t)}{\partial x} - \frac{\partial w(0, t)}{\partial x} &= -\int_0^x \frac{1}{1 + r_s^*(x')} \frac{\partial H(x', t)}{\partial x'}\, \mathrm{d}x' \\ &= -\frac{H(x, t)}{1 + r_s^*(x)} - \int_0^x \frac{H(x', t)\beta_s(x')}{[1 + r_s^*(x')]^2}\, \mathrm{d}x'. \end{aligned} \tag{32}$$

Further, we have

$$w(x,t) = w(0,t) + x\frac{\partial w(0,t)}{\partial x} - \int_0^x \frac{H(x',t)}{1+r_s^*(x')}\,\mathrm{d}x' - \int_0^x \int_0^{x''} \frac{H(x',t)\beta_s(x')}{[1+r_s^*(x')]^2}\,\mathrm{d}x'\,\mathrm{d}x'' \quad (33)$$

in which $\beta_s(x) = \mathrm{d}r_s^*(x)/\mathrm{d}x$, and $w(0,t)$ and $\partial w(0,t)/\partial x$ are the integral constants to be determined by the boundary conditions of the beam plates. For example, for the cantilevered beam plate shown in Figure 1, we recall the boundary condition of equation (14) $w(0,t) = \partial w(0,t)/\partial x = 0$. In this special case, equation (33) can be simplified by

$$w(x,t) = -\int_0^x \frac{H(x',t)}{1+r_s^*(x')}\,\mathrm{d}x' - \int_0^x \int_0^{x''} \frac{H(x',t)\beta_s(x')}{[1+r_s^*(x')]^2}\,\mathrm{d}x'\,\mathrm{d}x''. \quad (34)$$

Introducing

$$\hat{H}(x,t) = \frac{H(x-(x_1^*-[x_1^*])/2^n, t)}{1+r_s^*(x-(x_1^*-[x_1^*])/2^n)} \quad (35)$$

and applying equation (27) to equation (35), we can write

$$\hat{H}(x,t) \approx 2^{-n/2} \sum_{k=1-2N}^{2^n} \hat{H}\left(\frac{x_1^*+k}{2^n}, t\right)\phi_{n,k}(x). \quad (36)$$

Or equivalently,

$$\frac{H(x-(x_1^*-[x_1^*])/2^n, t)}{1+r_s^*(x-(x_1^*-[x_1^*])/2^n)} \approx 2^{-n/2} \sum_{k=1-2N}^{2^n} \frac{H([x_1^*]+k)/2^n, t)}{1+r_s^*(([x_1^*]+k)/2^n)}\phi_{n,k}\left(x+\frac{x_1^*-[x_1^*]}{2^n}\right). \quad (37)$$

Then translating the co-ordinate x and using equation (19), we obtain

$$\frac{H(x,t)}{1+r_s^*(x)} \approx \sum_{k=1-2N}^{2^n} \frac{H(([x_1^*]+k)/2^n, t)}{1+r_s^*(([x_1^*]+k)/2^n)}\phi_N(2^n x + x_1^* - [x_1^*] - k). \quad (38)$$

Similarly

$$\frac{H(x,t)\beta_s(x)}{[1+r_s^*(x)]^2} \approx \sum_{k=1-2N}^{2^n} \frac{H(([x_1^*]+k)/2^n, t)\beta_s(([x_1^*]+k)/2^n)}{[1+r_s^*(([x_1^*]+k)/2^n)]^2}\phi_N(2^n x + x_1^* - [x_1^*] - k). \quad (39)$$

Substitution of equations (38) and (39) into equation (33) leads to

$$w(x,t) = w(0,t) + x\frac{\partial w(0,t)}{\partial x} - \sum_{k=1-2N}^{2^n} \frac{H(([x_1^*]+k)/2^n, t)}{1+r_s^*(([x_1^*]+k)/2^n)} \int_0^x \phi_N(2^n x' + x_1^* - [x_1^*] - k)\,\mathrm{d}x'$$

$$- \sum_{k=1-2N}^{2^n} \frac{H(([x_1^*]+k)/2^n, t)\beta_s(([x_1^*]+k)/2^n)}{[1+r_s^*(([x_1^*]+k)/2^n)]^2} \int_0^x \int_0^{x''} \phi_N(2^n x' + x_1^* - [x_1^*] - k)\,\mathrm{d}x'\,\mathrm{d}x''. \quad (40)$$

Differentiation of equation (40) with respect to time variable t yields

$$\dot{w}(x,t) = \dot{w}(0,t) + x\frac{\partial \dot{w}(0,t)}{\partial x} - \sum_{k=1-2N}^{2^n} \frac{\dot{H}(([x_1^*]+k)/2^n, t)}{1 + r_s^*(([x_1^*]+k)/2^n)} \int_0^x \phi_N(2^n x' + x_1^* - [x_1^*] - k)\,\mathrm{d}x'$$

$$- \sum_{k=1-2N}^{2^n} \frac{\dot{H}(([x_1^*]+k)/2^n, t)\beta_s(([x_1^*]+k)/2^n)}{[1 + r_s^*(([x_1^*]+k)/2^n)]^2} \int_0^x \int_0^{x''} \phi_N(2^n x' + x_1^* - [x_1^*] - k)\,\mathrm{d}x'\,\mathrm{d}x'' \tag{41}$$

in which

$$H\left(\frac{[x_1^*]+k}{2^n}, t\right) = \sum_{m=1}^{[x_1^*]+k} q_m(t), \tag{42}$$

$$\dot{H}\left(\frac{[x_1^*]+k}{2^n}, t\right) = \sum_{m=1}^{[x_1^*]+k} \dot{q}_m(t) = \sum_{m=1}^{[x_1^*]+k} I_m(t). \tag{43}$$

Here, $[x_1^*]$ is the integer part of x_1^*. Noting that $([x_1^*]+k)/2^n$ is of the dyadic points, one can determine $H(([x_1^*]+k)/2^n, t)$ and $H(([x_1^*]+k)/2^n, t)$ at instant t using equations (42) and (43) in terms of the measurable electric charges $q_k(t)$ and electric current $I_k(t)$ in the sensing elements as long as we set $q_k = I_k = 0$ for $k < 0$, or $k > 2^n$. Hence, to determine the deflection $w(x,t)$ and velocity $\dot{w}(x,t)$, one needs to evaluate the integrals in equations (40) and (41), or equivalently, $\int_0^z \phi_N(y)\,\mathrm{d}y$ and $\int_0^z \int_0^{z'} \phi_N(y)\,\mathrm{d}y\,\mathrm{d}z'$. At an integer point $z = k$, the integrals can be determined precisely using the method of *connection coefficients* along with the properties of the scaling function $\phi_N(x)$ (see references [9, 11]). To evaluate the integrals in equations (40) and (41) at $z = 2^n x + x_1^* - [x_1^*] - k$ which are not integer points for $x = m/2^n$, we further approximate the integrals using an interpolating method and the values of integrals $\int_0^z \phi_N(y)\,\mathrm{d}y$ and $\int_0^z \int_0^{z'} \phi_N(y)\,\mathrm{d}y\,\mathrm{d}z'$ at integers: $z = m$. Through this procedure, equations (40) and (41) leads to the determination of the deflection and velocity as the sensing elements, $w(x_k, t)$ and $\dot{w}(x_k, t)(k = 0, 1, 2, \ldots, 2^n)$ in terms of the measurable electric charges $q_k(t)$ and the measurable electric currents $I_k(t)$ respectively. We will call these quantities of $w(x,t)$ and $\dot{w}(x,t)$ which are determined by equations (40) and (41) the measured deflection and the measured velocity of the plates respectively. In order to distinct them from those corresponding quantities of practical deformation of plate, from here on, we denote by $w^*(x,t)$ and $\dot{w}^*(x,t)$ to replace $w(x,t)$ and $\dot{w}(x,t)$ in equations (40) and (41) respectively.

5. CONTROL VOLTAGE APPLIED ON ACTUATORS

Here, a control law of negative feedback of the measured deflection and velocity signals is employed to determine the distribution of applied voltage across piezoelectric actuators. That is

$$f(x,t) = -G_1 w^*(x,t) - G_2 \dot{w}^*(x,t), \tag{44}$$

where $G_1 > 0$ and $G_2 > 0$ are the gain constants. The physical meaning of the control law of equation (44) implies that the first and the second terms are, respectively, corresponding to the increasing of rigidity and damping to the controlled structure through the control law.

Substituting equation (44) into equation (16), we get the governing equation for determining the control voltage $V(x, t)$ in the form

$$\frac{\partial^2 \{[1 + r_a^*(x)] V(x, t)\}}{\partial x^2} = G_1 w^*(x, t) + G_2 \dot{w}(x, t). \tag{45}$$

In order to give a distribution of control voltage $V(x, t)$, without loss of generality, we can employ the following boundary conditions to the differentiation equation (45)

$$V(0, t) = V(1, t) = 0 \tag{46}$$

which implies that zero voltage is applied at the ends of plate. It is evident that these conditions can be realized in practice. Thus, equations (45) and (46) constitute the boundary-value problem for distribution of applied control voltage across piezoelectric actuators following the measured signals of $w^*(x, t)$ and $\dot{w}^*(x, t)$. In order to get it, we will apply the wavelet Galerkin method/or weighted residual method (see reference [11]) to find the solution of the boundary-value problem of equations (45) and (46). From the expression of equation (27), one can write

$$V(x, t)[1 + r_a^*(x)] \approx 2^{-n/2} \sum_{k=k_1}^{k_2} V_k(t) \left[1 + r_a^*\left(\frac{x_1^* + k}{2^n}\right)\right] \phi_{n,k}(x), \tag{47}$$

$$w^*(x, t) \approx 2^{-n/2} \sum_{k=k_1}^{k_2} w_k^*(t) \phi_{n,k}(x), \tag{48}$$

$$\dot{w}^*(x, t) \approx 2^{-n/2} \sum_{k=k_1}^{k_2} \dot{w}_k^*(t) \phi_{n,k}(x), \tag{49}$$

where $V_k(t) = V((x_1^* + k)/2^n, t)$, $w_k^*(t) = w^*((x_1^* + k)/2^n, t)$, and $\dot{w}_k^*(t) = \dot{w}^*((x_1^* + k)/2^n, t)$. Substituting equations (47)–(49) into equation (45), and taking the base scaling functions of Haar's wavelet (see references [10, 11]) as the weighted functions of the weighted residual method to the resulting equation, we get

$$\sum_{k=k_1}^{k_2} 2^n [\phi_N'(j - k) - \phi_N'(j - k - 1)] \left[1 + r_a^*\left(\frac{x_1^* + k}{2^n}\right)\right] V_k(t)$$

$$= \sum_{k=k_1}^{k_2} \frac{1}{2^n} [G_1 w_k^*(t) + G_2 \dot{w}_k^*(t)] [\phi_N^{\int}(j - k) - \phi_N^{\int}(j - k - 1)]. \tag{50}$$

Here, $j = k_1 + 1, k_1 + 2, \ldots, k_2 - 1$, and the superscript prime "$'$" represents the differentiation with respect to variable x; and $\phi_N^{\int}(x) \equiv \int_{-\infty}^{x} \phi_N(x)\,\mathrm{d}x$. The values of $\phi_N'(x)$ and $\phi_N^{\int}(x)$ at integer points can be got by the method of *connection coefficients* (see references [9, 11]). Substitution of equation (47) into equation (46) leads to

$$\sum_{k=k_1}^{k_2} V_k(t) \phi_N(-k) = 0, \qquad \sum_{k=k_1}^{k_2} V_k(t) \phi_N(2^n - k) = 0 \tag{51, 52}$$

since

$$V(x, t) = 2^{-n/2} \sum_{k=1-2N}^{2^n} V_k(t) \phi_{n,k}(x). \tag{53}$$

can be gained by applying equation (27) to function $V(x, t)$. Equations (50)–(52) are a system of algebraic equations with unknowns $V_k(t)$. By solving this system of algebraic equations for $V_k(t)$, we get a continuous distribution of control voltage of equation (53). Since the applied voltage across a piezoelectric layer is a constant without varying with x in practice, we take the control voltage applied on the kth piezoelectric actuator, $\hat{V}_k(t)$, to be the average voltage within its corresponding interval: $[x_{k-1}, x_k]$, for $k = 1, 2, \ldots, 2^n$, i.e.,

$$\hat{V}_k(t) = 2^n \int_{(k-1)/2^n}^{k/2^n} V(x, t)\,\mathrm{d}t = \sum_{k=k_1}^{k_2} V_j(t)\,[\phi_N^{\mathrm{I}}(k-j) - \phi_N^{\mathrm{I}}(k-j-1)]. \tag{54}$$

Till now, the design of the control system of beam plates with piezoelectric sensors and actuators is completed by the wavelet theory.

It should be noted that this control approach based on the wavelet theory does not yield the phenomenon of control instability generated by the spilling over from those measurable signals and the actuation of those control voltage because the high order components of deformation beyond the main lobe of frequency band of $\phi_{n,k}(x)$ are almost auto-filtered by the expansions of equations (47)–(49) and (53) due to the characteristic of low-pass filter of the scaling function transform (see reference [11]). It is numerically found that the deformation of the plates within the main lobe of frequency band of $\phi_{n,k}(x)$ can be controlled using this approach.

6. NUMERICAL SIMULATIONS AND DISCUSSIONS (CASE STUDY)

6.1. PROGRAM OF NUMERICAL SIMULATIONS

The main steps of calculation taken in the numerical simulations are as follows:

(1) *Identification of deformed state of plate at time t*: According to equations (42) and (43), the values of $H(x, t)$ and $\dot{H}(x, t)$ at the dyadic points are obtained from the measurable signals of $q_k(t)$ and $I_k(t) = \dot{q}_k(t)$ on the piezoelectric sensors once the plate is deformed. Then, the measured deflection $w^*(x, t)$ and the measured velocity $\dot{w}^*(x, t)$ can be determined from equations (40) and (41) respectively.

(2) *Control voltage applied on piezoelectric actuators*: After the gains G_1 and G_2 are set, the control voltage on piezoelectric actuators is applied by the manner of output values of equations (53) and (54) after the boundary-value problem of equations (45) and (46) are solved by the wavelet Galerkin method or weighted residual method, i.e., to solve a system of algebraic equations (50)–(52) instead.

(3) *Equivalent transverse force and deformation simulation to the plate*: According to the model of equivalent bending deformation of a plate attached piezoelectric actuators on its surfaces [1, 4], the action of control voltage on piezoelectric actuators of the deformed plate can be equivalently replaced by a set of bending moments or couples. After that, from the theory of plates, one can give the equivalent transverse forces exerted on the mid-plane of plate. By means of the finite difference method for spatial part, and the Wilson-θ method for time part of the boundary-value problem of equations (13)–(15) with unknown deflection $w(x, t)$, we can gain the deformation state of $w(x, t)$ and $\dot{w}(x, t)$ at the node or dyadic points of plate to the next instant $t + \Delta t$, i.e., $w(x_k, t + \Delta t)$ and $\dot{w}(x_k, t + \Delta t)$, in which Δt is an increment step of time variable.

(4) *Response of controlled process*: According to equations (17) and (18), electric charge $q_k(t + \Delta t)$ and electric current $I_k(t + \Delta t)$ are measured from the piezoelectric sensors after $w(x, t + \Delta t)$ and $\dot{w}(x, t + \Delta t)$ were known by the above steps. Then, the

measurements $q_k(t)$ and $I_k(t)$ at instant t in the step (1) are, respectively, replaced by $q(t + \Delta t)$ and $I_k(t + \Delta t)$, and repeating steps (1)–(3), we can get a response of deflection of the controlled plate after it is excited by a disturbance either an initial deflection or an initial velocity or both of them at the initial instant $t = 0$.

6.2. NUMERICAL EXAMPLES

In order to show the efficiency and ability of the control program proposed in previous sections, firstly, a comparison of the numerical results from the program of this paper and those from the method of modal analysis in reference [8] to the controlled cantilevered beam-plate with constant thickness given in reference [8] is plotted in Figure 2 where the

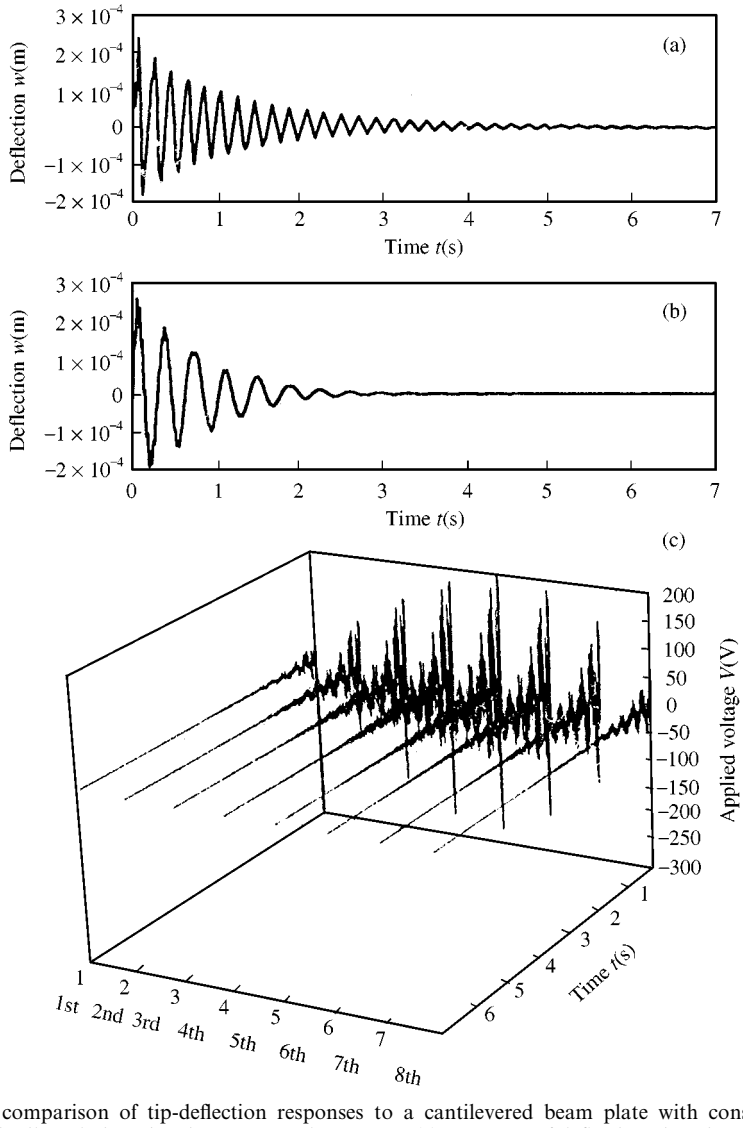

Figure 2. A comparison of tip-deflection responses to a cantilevered beam plate with constant thickness controlled by distributed piezoelectric sensors and actuators. (a) Response of deflection given in reference [8]. (b) Response of deflection in this paper. (c) Responses of control voltage applied on actuators in this paper.

TABLE 1

Parameters of materials and geometry in case study

Materials	Y (GPa)	ρ (kg/m^3)	μ	Thickness (mm)	Length (mm)	Width (mm)	e_{31} N/(V m)
Stainless steel	210	8000	0.3	2 (left) 1 (right)	300	20	
PVDF	2	1780	0.3	0.12	300	20	6×10^{-2}

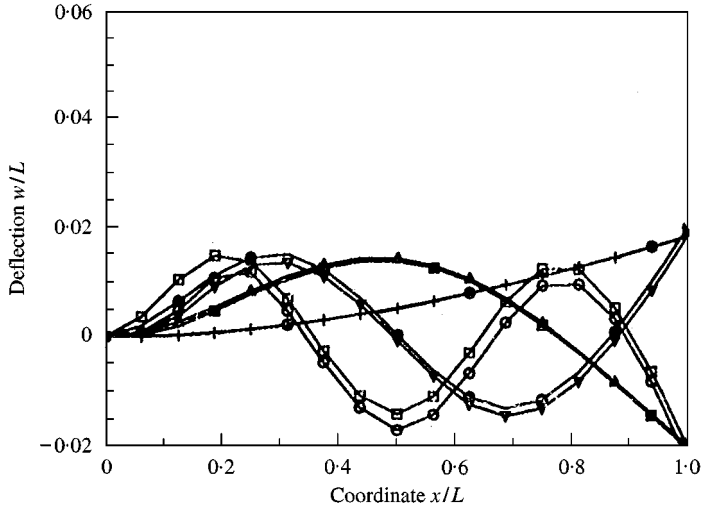

Figure 3. A comparison of deflections with free vibration modals and their identifications from equation (40) ($N = 5$, $n = 3$). Ex. = exact; Id. = identified: ●—● Ex. modal 1; +—+ Id. modal 1; ▲—▲ Ex. modal 2; ■—■ Id. modal 2; ●—● Ex. modal 3; ▼—▼ Id. modal 3; □—□ Ex. modal 4; ○—○ Id. modal.

responses of deflection at the free-end in the control progress is displayed. Here, Figure 2(a) shows the response given by reference [8] to the controlled plate with seven piezoelectric sensors and actuators, while Figure 2(b) exhibits one obtained by the control program of this paper to the same controlled structure and same initial impulse of 5×10^{-4} Ns on its free-end, to which eight piezoelectric sensors and actuators ($n = 3$) and the control parameters $G_1 = 0$, and $G_2 = 1{\cdot}0$ are employed. It is found that the duration of the control response from the initial disturbance to almost zero ($|w| < 10^{-6}$ m) is about 7 s in reference [8] while it is about 3·5 s in this paper. In Figure 2(c), the responses of applied voltage on the piezoelectric actuators corresponding to the control of Figure 2(b) are displayed. From it, it is found that the maximum applied voltage is less than 300 V, while it is given in reference [8] to be 280 V. Thus, these results tell us that the control approach proposed in this paper is efficiency. After that, a numerical simulation to a cantilevered beam plate with linearly variable thickness as shown in Figure 1 is carried out as a case study of the problems considered in this paper, whose parameters of materials and geometry are listed in Table 1.

Figure 3 displays a comparison of a deformed deflection with its identified one from equation (40) for $N = 5$ and $n = 3$, which exhibits a good accuracy to the identification. In the following simulations, we select the parameter $N = 5$ in the scaling function transform. The responses of the control voltage on each piezoelectric layer and the deflection at the free

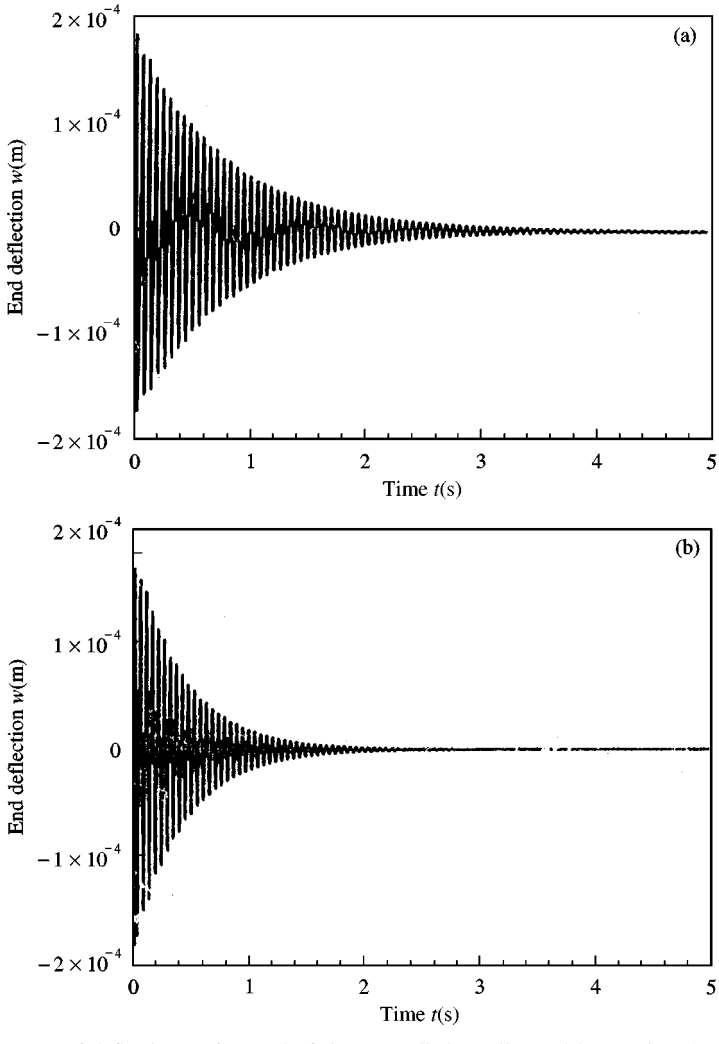

Figure 4. Responses of deflection at free end of the controlled cantilevered beam plate ($G_1 = 0$; $G_2 = 0{\cdot}10$). (a) $n = 2$ (corresponding to four piezoelectric elements). (b) $n = 3$ (corresponding to eight piezoelectric elements).

end of the plate, which is excited by an initial disturbance to the plate under a concentrated load of 0·03 N at the free end, are plotted in Figures 4 and 5 for the control parameters $G_1 = 0$ and $G_2 = 0{\cdot}1$. In Figures 4(a) and 5(a) are the responses for the case of resolution level $n = 2$, while Figures 4(b) and 5(b) are those for $n = 3$. From these results, one can find that the duration of suppressing the disturbance into almost zero for $n = 3$ is shorter than that for $n = 2$, while the control voltages applied on the piezoelectric actuators for these two cases are at the same level, when the control parameters G_1 and G_2 are taken one and the same. When we adjust the control parameter G_2 for the case of $n = 2$, the numerical simulations indicate that when G_2 increases up to $G_2 = 0{\cdot}2$, the duration decreases near to that for the case of $G_2 = 0{\cdot}1$ and $n = 3$, except that the control voltage doubly increases for the former case. Here, we should remind readers to note that there is a relation between the number, say S, of piezoelectric sensors/actuators and the resolution level n, i.e., $S = 2^n$. Next, the simulations for the initial disturbances with each one vibration modal among the former

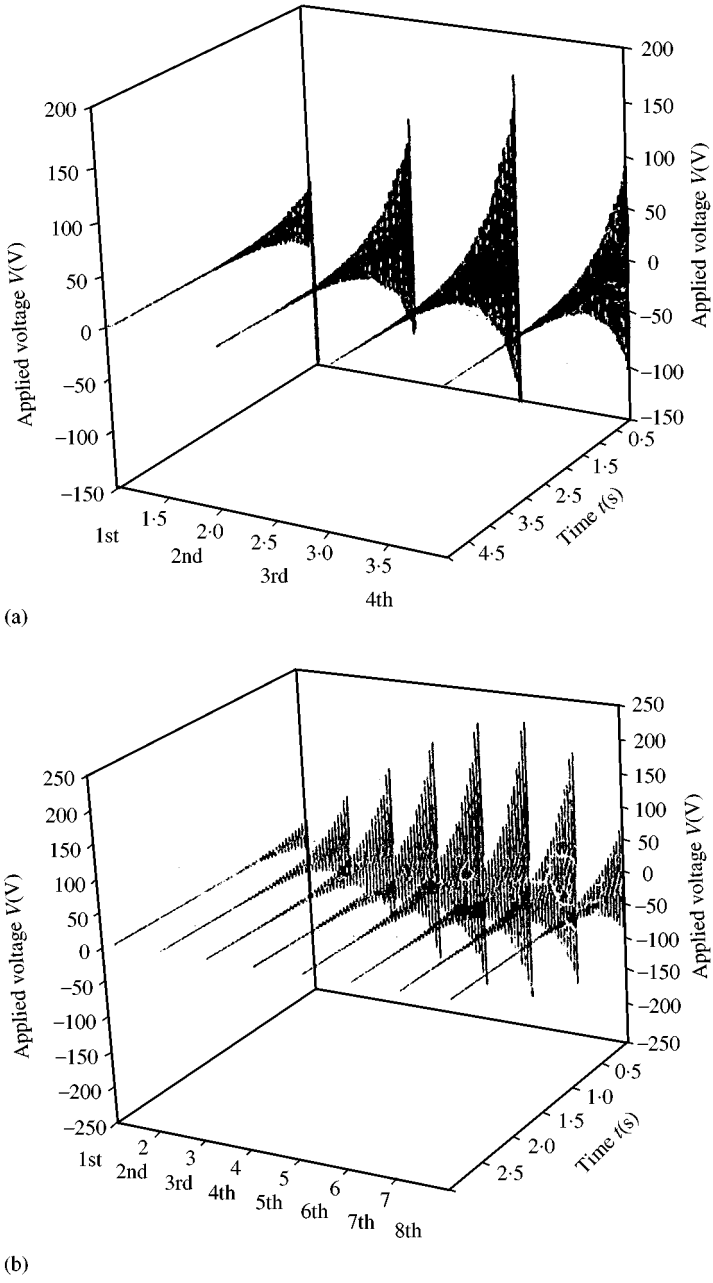

Figure 5. Responses of control voltage applied on piezoelectric actuators ($G_1 = 0$; $G_2 = 0{\cdot}10$). (a) $n = 2$ (corresponding to four piezoelectric actuators). (b) $n = 3$ (corresponding to eight piezoelectric actuators).

eight modals are performed for the case $n = 3$. The numerical results show that whether or not the disturbance is suppressed by the control system is dependent upon the piezoelectric elements employed. That is, the number of order of the disturbance which may be suppressed by the control programs may be equal to that of the piezoelectric elements 2^n. This is to say that when a disturbance is within the vibration modals of former 2^n order, the

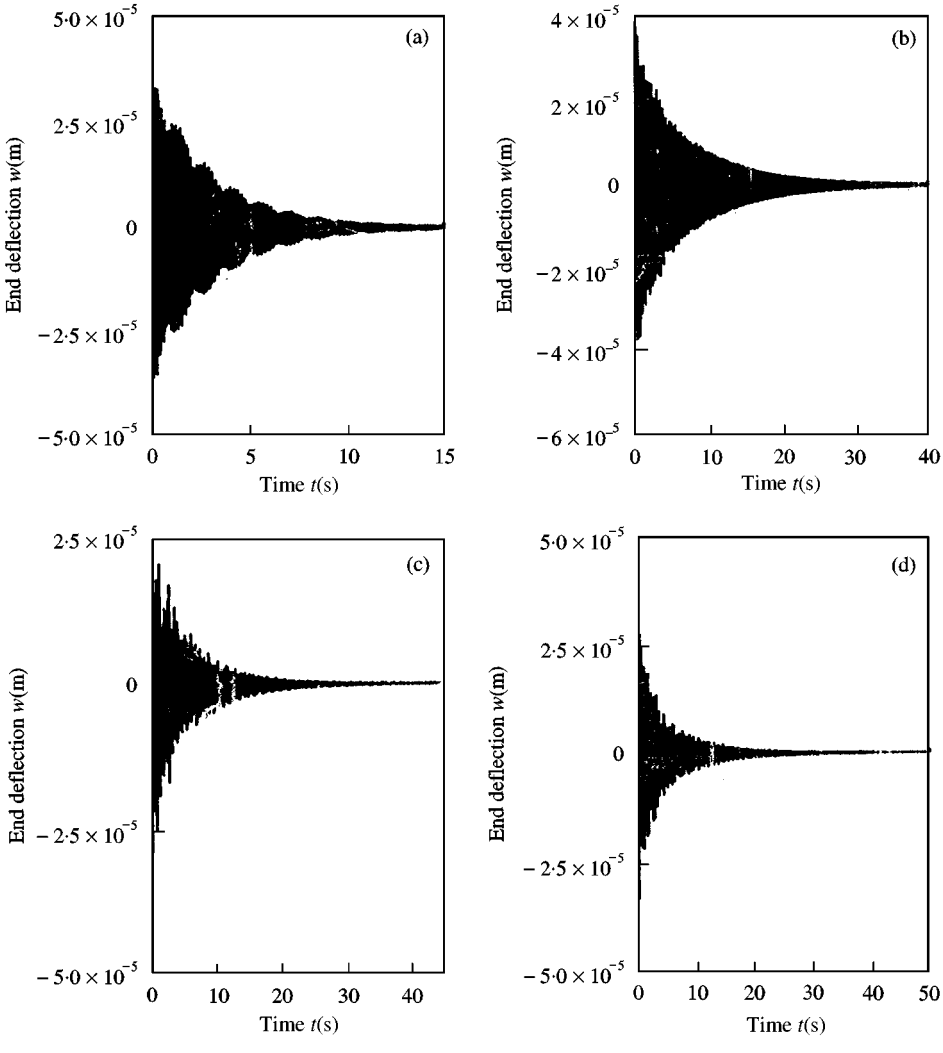

Figure 6. Responses of deflection at free end of the controlled plate disturbed by high order free vibrations ($n = 3$; $G_1 = 0$; $G_2 = 0{\cdot}10$). (a) Order 2. (b) Order 4. (c) Order 6. (d) Order 8.

disturbance may be suppressed by the control system with piezoelectric sensors/actuators 2^n. This conclusion can also shown by analysis of energy spectrum to which one can get that the spectrum of those suppressible disturbances with order m is within that of the base scaling functions with n-resolution level. Figure 6 plots the responses of the end deflection of the control plate with these initial disturbances of high order vibration modals, e.g., orders 2, 4, 6, and 8 when $n = 3$. It is clearly found that no higher vibration is excited in this control system when a relative low vibration modal is suppressed.

ACKNOWLEDGMENTS

This research work was supported by a grant of part from the National Natural Science Foundation of China (No. 19772014), and the National Science Foundation of China for

Outstanding Young Researchers (No. 19725207). The authors would like to give their sincere appreciation to these supports.

REFERENCES

1. H. S. TZOU and G. L. ANDERSON (editors) 1992 *Intelligent Structural Systems*. Boston: Kluwer Academic Publishers.
2. Y. Y. YU 1993 *Adaptive Structures and Material Systems* **35**, 185–195. Some recent advances in linear and nonlinear dynamical modeling of elastic and piezoelectric plates.
3. P. F. PAI, A. H. NAFEH, K. OH and D. T. MOOK 1993 *International Journal of Solids and Structures* **30**, 1603–1630. A refined nonlinear model of piezoelectric plate with integrated piezoelectric actuators and sensors.
4. H. S. TZOU and Y. H. ZHOU 1995 *Journal Sound and Vibration* **188**, 189–207. Dynamics and control of piezoelectric circular plates with geometrical nonlinearity.
5. H. S. TZOU and Y. H. ZHOU 1997 *Journal of Vibration and Acoustics, Transactions of the ASME* **119**, 382–389. Nonlinear piezothermoelectricity and multifield actuation, Part 2: Control of nonlinear buckling and dynamics.
6. Y. H. ZHOU and H. S. TZOU 2000 *International Journal of Solid and Structures* **37**, 1663–1677. Active control of nonlinear piezoelectric spherical shallow shells.
7. C. K. LEE 1992 Intelligent Structural System (Tzou and Anderson, editor), 75–167. Piezoelectric laminates: theory and experiments for distributed sensors and actuators. Boston: Kluwer Academic Publishers.
8. D. C. SUN, D. J. WANG and Z. L. XU 1997 *AIAA Journal* **35**, 583–584. Distributed piezoelectric segment method for vibration control of smart beams.
9. J. R. WILLIAM and K. AMARATUNGA 1994 *International Journal for Numerical Methods In Engineering* **37**, 2365–2388. Introduction to wavelet in engineering.
10. K. AMARATUNGA and J. WILLIAM 1994 *International Journal for Numerical Methods In Engineering* **37**, 2703–2716. Wavelet–Galerkin solution for one-dimensional partial differential equations.
11. R. L. MOTARD and B. JOSEPH 1994 *Wavelet Applications In Chemical Engineering*. Boston: Kluwer Academic Publishers.
12. J. Z. WANG and Y. H. ZHOU 1998 *Journal of Lanzhou University* (Natural Sciences Edition) **34**, 29–30. An error estimation of generalized Gaussian integral method in wavelet theory.